SEET ENGINEERING AND TECHNOLOGY JOURNAL

SEET Engineering and Technology Journal, 1 (issue), May (2026), page range
Journal homepage: https://www.seetfutoetj.ng/index.php/setj

Thermodynamic Modeling of *Gongronema Latifolium* Drying: Thin-Layer Models and Process Effects

Ukaoha, C. U.[1,*], Nwakuba, N. R.[2], Okorafor, O. O.[3], Asonye, G. U.[4], Alaka C. A.[5]
[1,2,3,4,5] Department of Agricultural and Bioresources Engineering, School of Engineering and Engineering Technology, Federal University of Technology, Owerri, Nigeria, P.M.B. 1056, Owerri, Imo State, Nigeria.

[*]Corresponding Author's E-mail: gukaoha@gmail.com

Abstract
The drying kinetics of Gongronema latifolium (*Utazi*) leaves were examined in this work under different drying conditions, such as temperature (40°C, 50°C, 60°C), airflow velocity (2.6 m/s, 3.6 m/s, 4.6 m/s), and leaf size (small (0.0028m^2), medium (0.0044cm^2), huge(0.0063m^2)). According to moisture ratio (MR) analysis, drying was expedited by greater temperatures and airflow velocities, with smaller leaves losing moisture more quickly. The Midili model was shown to be the most accurate model across various drying circumstances when seven empirical drying models were used to fit experimental data using curve fitting. The Wang and modified Page II models showed poor fit. The findings demonstrated that while leaf size was not significant ($p \geq 0.0665$), temperature and airflow was highly significant on drying behaviour ($p < 0.0001$). A 3D response surface analysis revealed that higher temperature and airflow improved desirability, resulting in optimal drying efficiency. With an R^2 value of 0.9870, the model showed excellent predictive accuracy, accounting for 98.7% of response variability. Reliability of the optimisation model was confirmed by experimental validation, which revealed a small error (3.78%) between simulated and observed shrinkage. By ensuring a balanced optimisation of drying conditions, the desirability function minimised energy consumption without sacrificing product quality. These results offer important new information for improving convective drying processes for agricultural products while maintaining both efficiency and quality.
Keywords: Drying kinetics, Moisture ratio, Empirical modelling, Shrinkage, Optimization, Response surface methodology

1. Introduction

A tried-and-true preservation technique that increases shelf life, lowers weight, and boosts storage and transportation effectiveness is crop drying (Bhardwaj et al., 2017). High energy consumption results from the process' heavy reliance on heat transfer to eliminate moisture. More than 85% of industrial dryers employ convective drying, which is nevertheless energy-intensive (Sabarez, 2015). Other methods, such radio frequency and microwave drying, have the potential to increase energy efficiency.

Essential nutrients and bioactive compounds that promote immune function are supplied by vegetables, which are essential to human health (Gupta, 2020). However, due to a lack of knowledge about their health advantages, green leafy vegetables (GLVs) like *utazi* are insufficiently utilised in rural Africa (Dada et al., 2021). Despite their economic, medicinal, and nutritional worth (Adeoye, 2020), they are extremely perishable due to their high moisture content (80–90% w.b.), which presents storage and value retention issues in Nigeria.

The drying behaviour of *Gongronema latifolium* (*Utazi*) in electric cabinet dryers under varying temperatures, air velocities, and leaf sizes is relatively unexplored. In agriculture, drying is crucial for increasing profitability, maintaining price stability, guaranteeing year-round availability, and fostering economic growth through job creation and market expansion. Food type, dryer design, and drying conditions all affect drying efficiency (Nwakuba et al., 2021). The choice of appropriate drying systems can be guided by optimising parameters like air temperature, velocity, humidity, and leaf size, which can lower energy consumption and enhance product quality. Literature over the past several years shows that efforts to optimise energy use as a means of enhancing the process variable of plant-based products have expanded globally (Adefemi and Ilesanmi, 2018; Aneke, Mbah, & Edeani, 2018; Nwakuba, 2018; Nwakuba, 2019; Ajuebor et al., 2022). Artificial techniques like hot air drying provide greater control but are frequently energy-intensive, whereas conventional sun drying is inexpensive but weather-dependent and quality-limiting.

Fruits and vegetables must be properly preserved because they are extremely perishable due to their 80–90% internal moisture content. Understanding the physicochemical changes that occur during drying is made more difficult by their complex structure. Texture, flavour, and drying kinetics are all impacted by shrinkage, a frequent occurrence during drying. Material characteristics, microstructure, and processing circumstances all have an impact on shrinkage (Mahiuddin et al., 2018). Because plant tissues are porous and hygroscopic, water migrates outward, significantly reducing their volume and affecting mechanical properties including torsional stiffness (Khan & Karim, 2017; Mahiuddin et al., 2018). Predictions of heat and mass transmission are more accurate when drying models take shrinkage into account.

To combat these obstacles, adjustment of drying parameters can be applied to optimise the percentage shrinkage of the *Utazi* samples while maintaining essential quality characteristics including colour, flavour, and nutrition. Understanding moisture loss, calculating drying time, and assessing the effects of temperature, leaf size, and air velocity are all made easier with the help of drying behaviour modelling. This study was motivated by the under-researched relationship between drying kinetics and process factors in leafy crops, despite its significance. A crucial technique for forecasting and improving drying processes is kinetic modelling, which characterises the rates of biochemical and physical changes

during drying (Inyang et al., 2018; Alara et al., 2018). For this reason, thin-layer drying models like Page, Newton, Henderson and Pabis, logarithmic, and Midilli–Kucuk are frequently used. By creating a predictive model for percentage shrinkage based on varying drying parameters and optimising conditions using the numerical desirability function, this work seeks to close the research gap. In order to determine the optimal convective drying conditions for premium *Utazi* preservation at the lowest possible energy cost, a Box-Behnken Design with a 3 × 3 factorial treatment was employed.

2. Materials and Methods

2.1 Leaf samples preparation

2.1.1 Preparation of sample

Fresh samples of *Utazi* leaves were collected from the vegetable farm located at Obinze, Owerri west LGA in Imo State, Nigeria. Following the division into three distinct size categories (0.0028 m^2 for small, 0.0044 m^2 for medium, and 0.0063 m^2 for large samples, with a tolerance range of ± 5%) by use of a meter rule, the samples underwent a cleaning process to eliminate any dirt. After the washing procedure, the initial mass of the samples was evaluated with the aid of a digital professional mini weighing balance (500/±0.01g) to establish a baseline for tracking moisture loss throughout the drying process, prior to their exposure to different drying conditions as outlined in the experimental plan.

2.1.2 Experimental procedure

The drying experiment was designed utilising a complete tool for experiment design, statistical analysis, and optimization. The software utilized was the Design-Expert® Statistical Package. The statistical software randomised the input values to decrease bias and experimental error (Table 1). Using the Box-Behnken Design technique, the drying trials were meticulously organised and the response surface was evaluated using the same. This decision was taken on purpose because it decreased the number of experimental runs needed while being notably effective at assessing the effects of numerous factors with three levels each. Under these circumstances, the Box–Behnken design type performs exceptionally well since it facilitates a rigorous examination of the experimental space. Additionally, plots of moisture ratio versus time graphs were fitted to the seven empirical thin-layer drying models in Matrix Laboratory (MATLAB 7.5.0 (R2007b)), where the model constants and statistical parameters were obtained to describe the drying behaviour.

Table 1: Experiment design layout.

Run	Temp (?)	Air Vel (m/s)	Leaf area (m^2)	Drying rate (g/h)	Shrinkage (%)
1	50	4.6	M		
2	50	3.6	M		
3	40	4.6	S		
4	60	3.6	M		
5	60	2.6	S		
6	60	4.6	S		
7	50	3.6	B		
8	50	3.6	S		
9	50	2.6	M		
10	40	4.6	B		
11	60	2.6	B		
12	60	4.6	B		
13	40	3.6	M		
14	40	2.6	B		
15	50	3.6	M		
16	40	2.6	S		
17	60	3.6	S		

To guarantee uniform conditions within the drying chamber, a laboratory-scale electric convective drier with controls for heat input and airflow rate was preheated for 35 minutes without any load prior to the experimental trials. A range of air temperatures (40, 50, and 60°C) and air velocities (2.6, 3.6, and 4.6 m/s) were used in the drying experiments, and all samples had an average ambient relative humidity of 29.7%. The dryer was first configured with the desired fan speed and air temperature (2.6 m/s and 40°C). For the purposes of even drying, the hot air was tangentially directed onto the leaf samples. During the trials, moisture loss was noted every ten minutes. The relative humidity inside the drying chamber was tracked using a thermo-hygrometer (HTC-1 Thermometer/Hygrometer). After the desired final moisture content was attained, each batch was stopped, and measurements were made of the drying time and total energy used (Nwakuba et al., 2021). There was additional documentation of changes in the *Utazi* leaf samples' physical attributes, including average mass and percentage shrinkage. Treatments were randomised to reduce the possibility of experimental errors. Three input parameters (leaf area, air temperature, and air velocity) were assessed at three levels, coupled with two response variables (drying rate and percentage shrinkage). Air temperature (40, 50, and 60°C), air velocity (2.6, 3.6, and 4.6 m/s), and leaf area (0.0028 (S), 0.0044(M), and 0.0063m^2(B)) were all systematically adjusted because they have a significant impact on the drying process (Nwakuba et al., 2021). At the same time, the drying rate and percentage shrinkage were meticulously measured and analysed. The experimental parameters are highlighted in Table 2, where the variables and levels are shown as −1, 0, and 1 in the coded and real versions, respectively, for low, medium, and high levels.

The observed responses, detailed in Table 2, include the drying rate (g/h) and per cent shrinkage (%). A total of 17 experimental runs were performed utilising prepared *Utazi* leaf samples dispersed over thin layers on aluminium mesh trays (77.5 cm × 43.3 cm) for drying experiments. Three air temperature settings (40, 50, and 60°C) were utilised with the trays placed in the electric convective drier to ensure warm air flowed axially over the leaf samples. These temperature ranges were chosen to optimize drying while maintaining the vegetables' flavour and nutritional content. An assortment of characteristics was tested to evaluate the thermal performance of the cross-flow air cabinet drier, including relative humidity, cabinet relative humidity, ambient air velocity, ambient air temperature, and cabinet air velocity. Temperature and relative humidity were measured using an exceptionally sensitive thermometer/hygrometer, while air velocity was assessed with an air-flow meter. The selected air velocities (2.6, 3.6, and 4.6 m/s) were meant to correlate with actual ambient air flow rates, establishing effective drying without displacing the leaves, which might lower thermal efficiency and waste useable heat. A hybrid thermometer/hygrometer was deployed to detect relative humidity and ambient air temperature (Table 1). Air velocities of 2.6 m/s (104V), 3.6 m/s (114V), and 4.6 m/s (143V)

Table 2: Arrangement of levels and experimental parameters.

Input parameter	Coded symbol	Factor level	
		Actual	Coded
Temperature (°C)	T	40	-1
		50	0
		60	1
Air velocity (ms^{-1})	V	2.6	-1
		3.6	0
		4.6	1
Leaf area ($x10^{-3}m^2$)	A	2.8	-1
		4.4	0
		6.3	1

were achieved by varying a variable resistor (NHT-4000, China) to supply particular voltages to a 1 hp AC motor within the heating system. Using an airflow meter (EXTECH 45170CM: 5-in-1 Environmental Meter), the air velocity during drying was measured and calibrated.

2.1.3 Data analysis and optimization process

To find statistically significant factors at $P < 0.05$, the data was analysed using analysis of variance (ANOVA). ANOVA and regression analyses were used to evaluate how well the quadratic polynomial model fit the drying data of *Gongronema latifolium*. Metrics like the coefficient of determination (R^2), adjusted R^2, predicted R^2, adequate precision, lack of fit, and coefficient of variation were among the metrics used. P-values were used to test model terms for every response parameter. Through the use of 3-D plots and response surface methodology (RSM) with Design Expert statistical software, the effects of several experimental parameters on percentage shrinkage were examined. Additionally, the moisture ratio was plotted versus time for various combinations of air velocity and leaf area at 60°C using Microsoft Excel. The quality of fit was evaluated using the correlation coefficient (R^2), sum of square errors (SSE), and root mean square error (RMSE). In order to ascertain the optimal goodness of fit, the values with the lowest SSE and RMSE as well as the highest R^2 were employed. Table 3 presents the empirical models together with their curve fitting equations.

Table 3: Mathematical models applied to thin layer drying of *Utazi* leaf(*Gongronema latifolium*).

S/N	Model Name	Model Equation
1	Newton/Lewis	$MR = exp(-kt)$
2	Page	$MR = exp(-kt^n)$
3	Modified Page II	$MR = exp\left(-k\left(\frac{t}{L^2}\right)^n\right)$
4	Henderson and Pabis	$MR = aexp(-kt)$
5	Logarithmic	$MR = aexp(-kt) + c$
6	Wang and Singh	$MR = M_0 + at + bt^2$
7	Midili *et al.*	$MR = aexp(-kt^n) + bt$

Source: (Inyang et al., 2018)

The primary and combined impacts of air velocity, drying air temperature, and leaf area at varying levels on the percentage shrinkage of *Utazi* leaf samples were optimised and evaluated using RSM optimisation, more especially the Box-Behnken design. By fitting mathematical models to experimental data, this approach aims to determine the best possible settings for the input variables that will minimise the response variable of interest. A desirability index (D^n) is used to statistically assess how well each output variable matches the intended goals. Additional experimental runs were conducted in triplicate under similar conditions to confirm the predicted optimal parameters, and the correlation between the mean outcomes of these trials was assessed. Equation (1) shows that the response variable (V_r) was defined using a second-order polynomial function, and the experimental data was evaluated using the least squares multiple regression approach.

$$V_r = \beta_0 + \beta_1 A + \beta_2 B + \beta_3 C + \beta_4 AB + \beta_5 AC + \beta_6 BC + \beta_7 A^2 + \beta_8 B^2 + \beta_9 C^2 \quad (1)$$

Where: *A, B, and C* are the independent variables, which are air temperature (°C), air velocity (m/s), and sample area (m^2), respectively; β_0 denotes the model intercept; and V_r is the response variable, which includes drying rate in (g/h), and shrinkage (%). Regression coefficients include $\beta_1, \beta_2, \beta_3, \beta_4, \beta_5, \beta_6, \beta_7, \beta_8$, *and* β_9. The linear effects are represented *by* $\beta_1 A$, $\beta_2 B$, and $\beta_3 C$; the interaction or cross-product effects are represented by $\beta_4 AB$, $\beta_5 AC$, and $\beta_6 BC$; and the quadratic or curvature effects are represented by $\beta_7 A^2$, $\beta_8 B^2$, and $\beta_9 C^2$ (Nwakuba, 2019).

2.2 Basic theory

2.2.1 Moisture ratio (dimensionless)

The moisture content data that has been calculated in the experiment will be converted into a humidity ratio. This will be used for model analysis and computation. The moisture ratio (MR) can be defined by Equation (2) (Kusuma *et al.*, 2023) as:

$$MR = \frac{M_t - M_e}{M_o - M_e} \quad (2)$$

Where; *MR = Moisture ratio,* M_t *= moisture content at time t (%),* M_o *= initial moisture content (%),* M_e *= equilibrium moisture content (%).*

However, the moisture ratio was calculated using Equation (3) in place of Equation (2) due to the continuous fluctuation in the relative humidity during the drying processes (Alara *et al.*, 2018b).

$$MR = \frac{M_t}{M_0} \quad (3)$$

Where; M_t *= moisture content at time t (%),* M_o *= initial moisture content (%).*

2.2.2 Drying rate (D_R)

The drying rate was determined by measuring the amount of moisture removed from the *Utazi* leaf sample over a specified time interval (h). The moisture loss (M_L) is represented in Equation 4 as:

$$M_L = W_i - W_f \quad (4)$$

Where*;* W_i*= initial weight, and* W_f *= final weight.*

Consequently, the drying rate is represented by Equation 5 as:

$$D_R(g/h) = \frac{M_L}{t} \quad (5)$$

2.2.3 Shrinkage ratio

Shrinkage usually denotes sample volume change after/during drying to the initial volume (Mutuli *et al.*, 2020). In the conventional drying method (hot air drying), the changes in the shape of the sample are concentrated in length and breadth. The shrinkage ratio (SR) was measured in order to estimate the volume changes of the dried samples. SR of the dried sample was expressed in Equation (6) (Huang and Zhang, 2016) as:

$$SR = \frac{L_i - L_f}{L_i} * 100 \quad (6)$$

Where*;* L_i *= initial length (cm), and* L_f *= final length (cm).*

3.0 Result and Discussion

3.1 Drying kinetics

Figure 1 shows the variation in moisture ratio (MR) over time for *utazi* leaves under various drying conditions, such as leaf size (small, medium, and large), temperature (40°C, 50°C, and 60°C), and air velocity (2.6 m/s, 3.6 m/s, and 4.6 m/s). All samples start off with an MR of 1, which indicates full moisture content. As a result of drying, this value gradually drops. Moisture loss is accelerated by higher temperatures and air velocities; the fastest drying rates are achieved at 60°C and 4.6 m/s. Larger leaves lose moisture more slowly than smaller ones, most likely as a result of structural variations and retention capacity. According to Nwakuba et al. (2021), the drying pattern exhibits a distinctive trend, starting with a quick loss of moisture and then gradually declining to equilibrium. Greater surface areas facilitate the diffusion of moisture, which shortens drying times and increases energy efficiency. According to Idlimam et al. (2007), drying kinetics are greatly influenced by temperature.

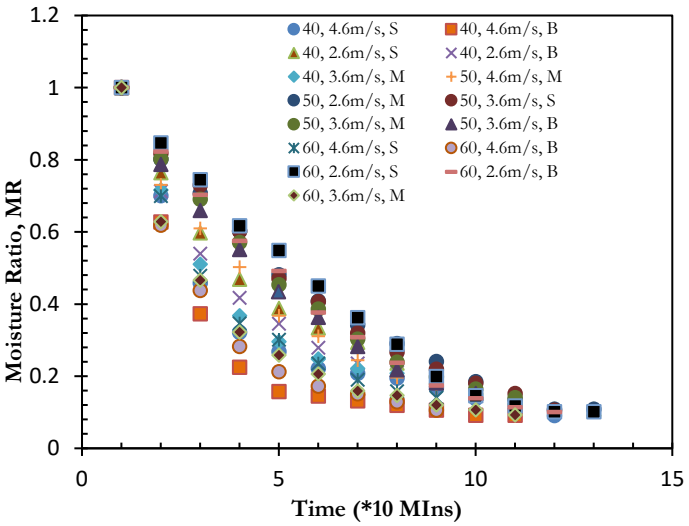

Figure 1: Moisture ratio variation versus drying duration at various drying conditions (Temperature, air velocity and leaf size).

3.2 Curve Fitting of Drying Data

Tables 4, 5 and 6 provides an overview of the drying outcomes derived from the model statistics, with reference to the statistical parameters (R^2, RMSE, and SSE) derived from the moisture ratio versus drying time curve-fitting computations for the seven empirical thin-layer drying models that were chosen. Overall, the statistical parameters show good fits with values ranging from $-0.04711 \leq R^2 \leq 0.999$, $0.3045 \leq RMSE \leq 0.01012$, and $0.9274 \leq SSE \leq 9.224*10^{-4}$.

The Midili model demonstrated the highest degree of accuracy and best described the drying properties of *Utazi* at an air velocity of 3.6 m/s, according to the data shown in Table 4 of the summary about the drying model coefficients at 40°C. On the other hand, the Wang model was judged to be the least suitable for explaining *Utazi's* drying behaviour at 3.6 m/s because it showed the worst fit. Table 5 makes it clear that the Henderson and Pabis model performs exceptionally well in predicting the drying characteristics of *utazi* at 50°C, especially when samples with large leaf areas are considered. However, when applied to these drying settings, the modified Page II model shows a suboptimal fit, suggesting that it is not very good at precisely describing the *Utazi's* drying behaviour in these particular conditions. The Midili model outperformed the others in forecasting the drying characteristics of *Utazi* with a medium leaf area at 3.6 m/s air velocity and at 60°C, as shown by the results in Table 6. However, the modified Page II model performed the worst under the specified conditions and is not recommended for forecasting *Utazi's* drying behaviour at higher temperatures.

The top two mathematical models for predicting the moisture ratio (MR) of *Utazi* leaves at three distinct drying temperatures—40°C, 50°C, and 60°C—are shown in Table 7. With values ranging from 0 (totally dry) to 1 (fully hydrated), the moisture ratio (MR) shows how much moisture remaining in the leaves over time. Every model is shown in both its general form and as a fitted equation with constants that have been determined through experimentation. At 40°C, the Midili model was discovered to be among the most accurate forecasters. This model may capture complex drying behaviour because it combines a linear correction factor with an exponential decay term. The logarithmic model was the second-best model at this temperature. An offset term (c) is included in the fitted version to account for any moisture that was not completely eliminated during drying. With its simplified exponential form, the Henderson and Pabis model demonstrated good performance at 50°C, suggesting near-complete initial moisture ($a \approx 1$) and a gradual decay rate. Additionally, the logarithmic model fit well. It is a significantly improved version of the Henderson and Pabis model by the minor offset ($c \approx 0.0035$), which indicates little residual moisture. The Midili model was once again shown to be among the best for drying at 60°C. As the temperature rises, moisture is lost more quickly, as seen by the higher decay constant ($k = 0.0736$) than at 40°C. This model's purely exponential form with a time exponent ($n = 0.7107$) suggests non-uniform drying behaviour. The time exponent ($n = 0.7107$) in the strictly exponential form of this model indicates non-uniform drying behaviour. In summary, the most effective models change with temperature; Henderson and Pabis are simpler models that perform well in moderate drying circumstances, while Midili and Logarithmic models are more flexible at lower and higher temperatures. The drying kinetics of *Utazi* leaves are best described by some models that include time exponents (n) and offset terms (c). The differences in model selection by temperature demonstrate how drying circumstances affect the kinetics of moisture loss, with Page appearing as a powerful predictor at higher temperatures and more complicated models like Midili doing better at lower temperatures.

Table 5 *Utazi* at 50°C, 3.6m/s.

S/N	Model Name	Size	Constants							R^2	RMSE	SSE
			a	b	c	k	l	M_0	n			
1	Newton/Lewis	S				0.01848				0.9968	0.01658	0.003299
		M				0.01976				0.9982	0.01231	0.001817
		B				0.02095				0.9986	0.0107	0.001375
2	Page	S				0.01435			1.062	0.998	0.01378	0.00209
		M				0.01824			1.02	0.9983	0.0124	0.001691
		B				0.02161			0.9922	0.9987	0.0111	0.001355
3	Henderson and Pabis	S	1.012			0.01872				0.997	0.01662	0.003038
		M	0.9999			0.01976				0.9982	0.01285	0.001818
		B	0.9947			0.02083				0.9987	0.01098	0.001327
4	Midili	S	1	$2.94*10^{11}$		0.01848			1	0.9968	0.01732	0.003299
		M	1	$1.86*10^{12}$		0.01976			1	0.9982	0.01231	0.001817
		B	0.9961	$3.27*10^{05}$		0.021			1	0.9987	0.01206	0.00131
5	Wang and Singh	S	-0.01457	$6.14*10^{05}$				0.9819		0.9975	0.01589	0.002524
		M	-0.01506	$6.60*10^{05}$				0.9686		0.9969	0.01763	0.00311
		B	-0.01575	$7.24*10^{05}$				0.9629		0.9966	0.0186	0.003458
6	Logarithmic	S	1		$9.23*10^{05}$	0.01848				0.9968	0.01732	0.003299
		M	1		0.000491	0.01979				0.9982	0.01289	0.001827
		B	0.9922		0.003456	0.02101				0.9987	0.01149	0.001319
7	Modified Page II	S				0.001628	0.001341		0.374	0.7773	0.1509	0.2277
		M				0.02009	1		0.9959	0.9982	0.01306	0.001875
		B				0.001797	0.001676		0.3838	0.815	0.1371	0.1879

Table 4 *Utazi* 40°C, 3.6m/s.

S/N	Model Name	Size	Constants							R^2	RMSE	SSE
			a	b	c	k	l	M_0	n			
1	Newton/Lewis	M				0.02689				0.9581	0.05509	0.03642
2	Page	M				0.07544			0.7277	0.9919	0.02527	0.007025
3	Henderson and Pabis	M	0.933			0.02481				0.9654	0.05233	0.03012
4	Midili	M	1	0.000581		0.05394			0.8469	0.995	0.02083	0.004339
5	Wang and Singh	M	-0.01684	$9.01*10^{05}$				0.8857		0.9462	0.06837	0.04674
6	Logarithmic	M	0.8793		0.1163	0.03858				0.995	0.02084	0.004342
7	Modified Page II	M				2.325	10.54		0.7278	0.9919	0.0265	0.007025

Table 7 Summary table of the two best-performing models at varying temperatures

SUMMARY TABLE FOR *UTAZI* INDICATING THE BEST 2 MODELS AT 40°C			
S/N	Model name	General equation	Actual model
1	Midili	$MR = ae(-kt^n) + bt$	$MR = e^{(-0.0539t^{0.8469})+0.000581t}$
2	Logarithmic	$MR = ae(-kt) + c$	$MR = 0.8793e^{(-0.03858t)+0.1163}$
SUMMARY TABLE FOR *UTAZI* INDICATING THE BEST 2 MODELS AT 50°C			
1	Henderson and Pabis	$MR = ae(-kt)$	$MR = 0.9947e^{(-0.02083t)}$
2	Logarithmic	$MR = ae(-kt) + c$	$MR = 0.9922e^{(-0.02101t)+0.003456}$
SUMMARY TABLE FOR *UTAZI* INDICATING THE BEST 2 MODELS AT 60°C			
1	Midili	$MR = ae(-kt^n) + bt$	$MR = e^{(-0.0736t^{0.7979})+0.0003868t}$
2	Page	$MR = e(-kt^n)$	$MR = e^{(-0.09447t^{0.7107})}$

Table 6 *Utazi* 60°C, 3.6m/s.

S/N	Model Name	Size	Constants							R^2	RMSE	SSE
			a	b	c	k	l	M_0	n			
1	Newton/Lewis	M				0.03305				0.9646	0.05115	0.0314
2	Page	M				0.09447			0.7107	0.9972	0.01514	0.002522
3	Henderson and Pabis	M	0.9319			0.03048				0.9712	0.04817	0.02552
4	Midili	M	1	0.0003868		0.07396			0.7979	0.999	0.01012	0.0009224
5	Wang and Singh	M	0.01779	$9.90*10^{05}$				0.8556		0.9398	0.05332	0.05332
6	Logarithmic	M	0.8927		0.08909	0.0435				0.9961	0.01848	0.003417
7	Modified Page II	M				0.6983	0.005131		0.3214	-0.04711	0.3045	0.9274

3.3 Shrinkage (ψ)

The relationship between shrinkage (%) and two independent variables—temperature (°C) and airflow (m/s)—is depicted in the 3D surface map (Figure 2). The upward slope of the surface indicates that the shrinkage percentage rises with temperature and airflow. This pattern is clearly represented by the colour gradient, which moves from blue (low shrinkage) to yellow and red (high shrinkage). Increased airflow promotes convective drying, which intensifies shrinkage, while higher temperatures hasten moisture loss, which causes greater structural collapse. Actual experimental values are represented by the depicted data points (red circles), some of which are above and below the expected surface. The contour map shows the distribution of shrinkage across temperature and airflow changes in two dimensions. This analysis is essential for optimizing drying conditions to balance moisture removal while minimizing excessive shrinkage, which affects product quality and texture. These visual trends are consistent with the ANOVA findings, which show that temperature has a highly significant impact on shrinkage ($p < 0.0001$) and that airflow also plays a substantial ($p < 0.0001$), albeit smaller, role.

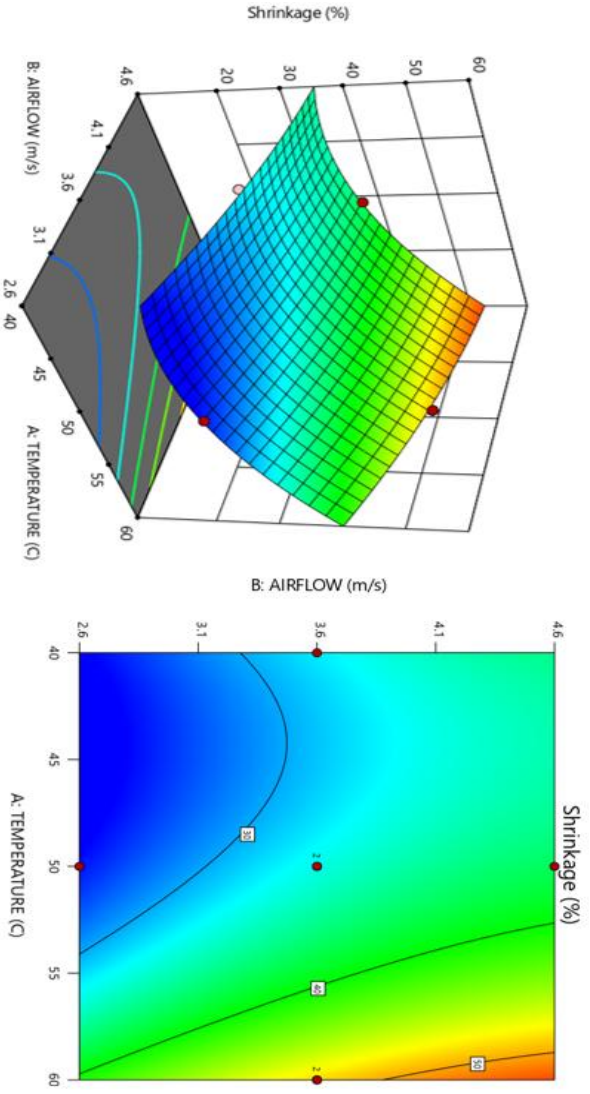

Figure 2: Impact of process conditions (airflow and temperature) on the percentage shrinkage of *Utazi* leaf (a) Three-dimensional plot (b) Contour plot.

Temperature and airflow have a substantial impact on the drying process, according to the ANOVA results (Table 8), but leaf area has a small but statistically insignificant effect ($p = 0.0665$). The results of an experimental study by Putra & Ajiwiguna (2017) on the impact of air temperature and velocity on the drying process are likewise in line with this. The model's F-value of 58.88 indicates that it successfully explains the majority of the variation in the data, making it highly significant ($p < 0.0001$). With the biggest sum of squares (722.37), temperature is the most significant element. Airflow comes in second (345.74), both of which have strong statistical significance ($p<0.0001$). The significant quadratic term for temperature suggests there may be an optimal temperature range beyond which additional increases provide diminishing returns . The fact that the quadratic terms for airflow and leaf area, as well as the interaction terms (TV, AT, and AV), are negligible indicates that these variables operate independently. Despite the relatively low residual sum of squares (17.65), it is challenging to completely evaluate model fit because pure error (0.0000) is absent. Overall, airflow and temperature are the most important variables to optimise, and process management is made easier by the absence of significant interactions. The percentage shrinkage of *Utazi* is thus accurately predicted by the relationship that is articulated and expressed in coded terms in Equation (7). the equation demonstrates a significant correlation between the observed and predicted data, accounting for 98.7% of the variation in the response variable with an R^2 value of 0.9870. The model's excellent R^2 shows that it can reliably and precisely forecast drying behaviour in a variety of situations. This outcome is consistent with research by Sturm et al. (2014), which showed that temperature, humidity, and airflow levels during drying processes significantly influence shrinkage. In a similar vein, their analysis of how process management techniques affected the drying kinetics, colour, and shrinkage of air-dried apples highlighted how critical temperature is in determining shrinkage results. Consequently, an accurate forecast of the *Utazi* leaf percentage shrinkage is obtained from the relationship that is stated and expressed in coded terms. A 2nd-order quadratic model is entirely suitable for forecasting the percentage shrinkage from experimental data, according to equation (7), which is also in line with the findings of (Uzoma et al., 2020).

Table 8: Analysis of variance for *Utazi* percentage shrinkage.

Source	Sum of Squares	df	Mean Square	F-value	p-value	
Model	1335.86	9	148.43	58.88	< 0.0001	significant
T-TEMPERATURE	722.37	1	722.37	286.57	< 0.0001	"
V-AIRFLOW	345.74	1	345.74	137.16	< 0.0001	"
A-LEAF AREA	11.88	1	11.88	4.71	0.0665	n.s
TV	0.3160	1	0.3160	0.1254	0.7337	"
AT	0.3655	1	0.3655	0.1450	0.7147	"
AV	3.55	1	3.55	1.41	0.2740	"
T^2	155.96	1	155.96	61.87	0.0001	significant
V^2	8.67	1	8.67	3.44	0.1061	n.s
A^2	2.03	1	2.03	0.8059	0.3992	"
Residual	17.65	7	2.52			
Lack of Fit	17.65	5	3.53			
Pure Error	0.0000	2	0.0000			
Cor Total	1353.50	16				

$$\psi = 33.13 + 8.22T + 5.88V + 1.09A + 0.1988TV - 0.2137AT + 0.6663AV + 7.10T^2 - 1.75V^2 + 0.8449C^2 \quad (R^2=0.9870) \quad (7)$$

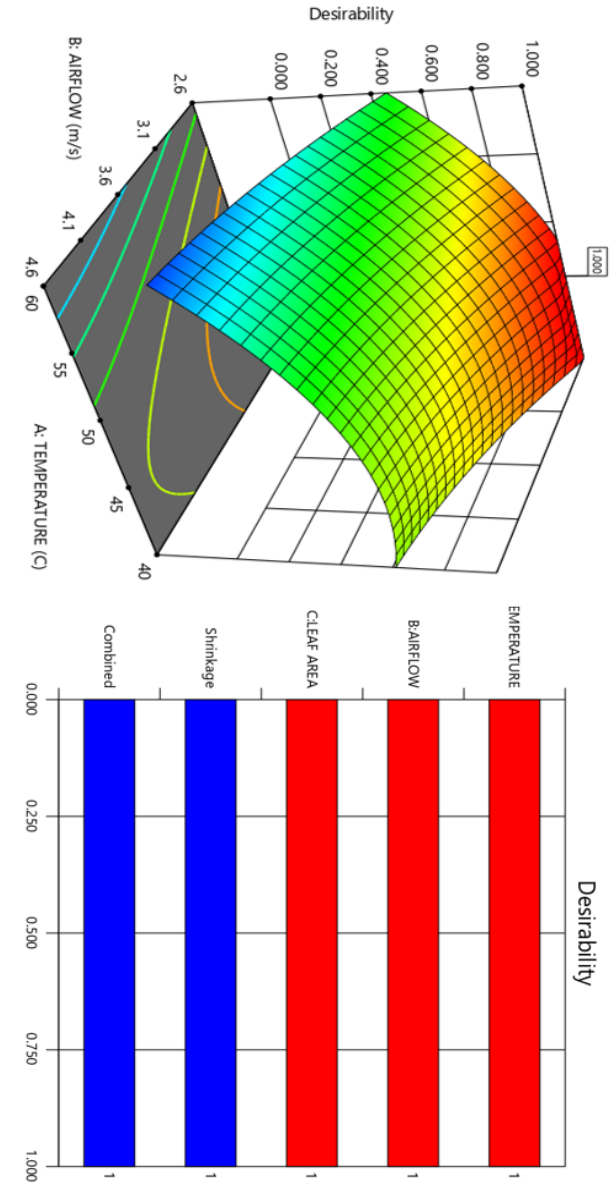

Figure 3: (a) Joint desirability RSM plot **(b)** Optimized desirability values of input, response, and collective parameters for *Utazi* leaf.

Table 6: Desirability limit for optimal dryer operation of *Utazi*.

Source	Input parameters				(Dⁿ)
	T(°C)	V(m/s)	A(m²)	ψ (%)	
Simulated	46.67	2.6	Medium	24.03	1
Experimental				25.69	
Error				3.78	

4.0. Conclusion

The study shows that the drying kinetics of *Utazi* leaves are significantly influenced by temperature, airflow, and leaf size. Moisture loss is accelerated by higher temperatures and airflow rates; fastest drying periods are achieved at 60°C and 4.6 m/s. Because they have a higher surface-area-to-volume ratio, which promotes moisture diffusion, smaller leaves lose moisture more quickly than bigger ones. Rapid initial moisture loss is a hallmark of the drying process, which progressively stabilises when equilibrium is attained. These results are consistent with earlier studies, demonstrating that temperature has the greatest impact on drying behaviour.

According to curve-fitting studies, different drying models function best in different scenarios. The Henderson and Pabis model did well at 50°C, but the Midili model consistently gave the greatest fit at various temperatures and airflow rates, especially at 40°C and 60°C. On the other hand, under the majority of circumstances, the Wang and Modified Page II models had poor prediction accuracy. Strong model performance is indicated by the statistical parameters (R^2, RMSE, and SSE), confirming the model's applicability in forecasting the drying properties of *Utazi* leaves. The variations in model effectiveness across drying conditions highlight the need for condition-specific model selection to ensure accurate predictions.

Temperature and airflow are the main parameters influencing drying efficiency and shrinkage, as further supported by the 3D response surface and ANOVA results. While airflow promotes convective drying, higher temperatures cause structural collapse from moisture loss, which increases shrinkage. The best drying conditions are determined by the desire index analysis, which maximises moisture removal while maintaining structural integrity. The close agreement between simulated and experimental shrinkage values, with an error margin of less than 5%, demonstrates the model's remarkable predictive performance.

All things considered, this study offers insightful information about optimising *Utazi* leaf drying, highlighting the significance of choosing suitable drying conditions and mathematical models. In the agricultural and food processing sectors, the results can be used to increase drying efficiency, lower energy usage, and preserve product quality. To improve drying models and optimisation techniques, future studies should examine other variables including humidity and drying time.

Declaration Statement

The authors agreed with total interest to submit the manuscript entitled, 'Thermodynamic Modeling of *Gongronema Latifolium* Drying: Thin-Layer Models and Process Effects' for publication in your reputable Institution without conflict of interest be it design and implementation, respect towards society, resources and research output and conduct without deceptive acts.

Conflict of Interest

The authors declare no conflict of interest.

Author Contribution

Ukaoha Collins U.: Conceptualization; data curation; formal analysis; methodology; software; supervision; validation; writing-original draft; writing-review & editing. **Nwakuba Nnaemeka R.:** Formal analysis; investigation; methodology; writing-review & editing, methodology; software; supervision. **Okorafor Okey O.:** Conceptualization; formal analysis; investigation; methodology; supervision. **Asonye Gladys U:** writing-review & editing;

methodology. **Alaka Chinomso A.:** Software; methodology; editing.

References

Adefemi, A. O., & Ilesanmi, D. A. (2018). Development and Optimisation of Drying Parameters for Low-Cost Hybrid Solar Dryer Using Response Surface Method. *Journal of Sustainable Bioenergy Systems*, *08*(02), 23–35. doi: 10.4236/jsbs.2018.82002

Adeoye, I. B. (2020). Factors Affecting Efficiency of Vegetable Production in Nigeria: A Review. In *Agricultural Economics*. Intech Open. https://doi.org/10.5772/intechopen.92702

Ajuebor, F., Aworanti, O. A., Agbede, O. O., Agarry, S. E., Afolabi, T. J., & Ogunleye, O. O. (2022). Drying Process Optimization and Modelling the Drying Kinetics and Quality Attributes of Dried Chili Pepper (Capsicum frutescens L.). *Trends in Sciences*, *19*(17), 5752–5752. doi: 10.48048/tis.2022.5752

Alara, O. R., Abdurahman, N. H., & Olalere, O. A. (2018a). Ethanolic extraction of bioactive compounds from Vernonia amygdalina leaf using response surface methodology as an optimization tool. *Journal of Food Measurement and Characterization*, *12*(2), 1107–1122. https://doi.org/10.1007/s11694-018-9726-3

Alara, O. R., Abdurahman, N. H., & Olalere, O. A. (2018b, June 1). *(2) (PDF) Mathematical modelling and morphological properties of thin layer oven drying of Vernonia amygdalina leaves*. ResearchGate. https://www.researchgate.net/publication/319618649_Mathematical_modelling_and_morphological_properties_of_thin_layer_oven_drying_of_Vernonia_amygdalina_leaves

Aneke, N. A. G., Mbah, G. O., & Edeani, N. J. (2018). Response Surface Methodology For optimisation of hot air drying of water yam slices. *International Journal of Scientific and Research Publications (IJSRP)*, *8*(8). https://doi.org/10.29322/IJSRP.8.8.2018.p8030

Bhardwaj, A. K., Chauhan, R., Kumar, R., Sethi, M., & Rana, A. (2017). Experimental investigation of an indirect solar dryer integrated with phase change material for drying valeriana jatamansi (medicinal herb). *Case Studies in Thermal Engineering*, *10*, 302–314. https://doi.org/10.1016/j.csite.2017.07.009

Dada, T. E., Otitoloju, K., Adjonu, R., Crockett, J., & Nwose, E. U. (2021). Nutritional and medicinal values of common green leafy vegetables consumed in Delta State, Nigeria: A review. *International Journal of Community Medicine and Public Health*, *8*(5), 2564–2571. https://doi.org/10.18203/2394-6040.ijcmph20211789

Gupta, A. (2020). Green leafy vegetables source of nutrients: A review. *The Pharma Innovation Journal*. https://www.academia.edu/71985485/Green_leafy_vegetables_source_of_nutrients_A_review

Huang, J., & Zhang, M. (2016). Effect of three drying methods on the drying characteristics and quality of okra. *Drying Technology*, *34*(8), 900–911. https://doi.org/10.1080/07373937.2015.1086367

Idlimam, A., Ethmane, K. C. S., & Kouhila, M. (2007). Single layer drying behaviour of grenade peel in a forced convective solar dryer. Revue Des Energies Renouvelables, 10(2), 191–203.

Inyang, U. E., Oboh, I. O., & Etuk, B. R. (2018). Kinetic Models for Drying Techniques—Food Materials. Advances in Chemical Engineering and Science, 8(2), Article 2. https://doi.org/10.4236/aces.2018.82003

Khan, Md. I. H., & Karim, M. A. (2017). Cellular water distribution, transport, and its investigation methods for plant-based food material. Food Research International, 99, 1–14. https://doi.org/10.1016/j.foodres.2017.06.037

Kusuma, H. S., Lantip, G. I. A., Mutiara, X., & Iqbal, M. (2023). Evaluation of Mini Bibliometric Analysis, Moisture Ratio, Drying Kinetics, and Effective Moisture Diffusivity in the Drying Process of Clove Leaves using Microwave-Assisted Drying. Applied Food Research, 3(1), 100304. https://doi.org/10.1016/j.afres.2023.100304

Mahiuddin, M., Khan, Md. I. H., Kumar, C., Rahman, M. M., & Karim, M. A. (2018). Shrinkage of Food Materials During Drying: Current Status and Challenges. Comprehensive Reviews in Food Science and Food Safety, 17(5), 1113–1126. https://doi.org/10.1111/1541-4337.12375

Mutuli, G. P., Mbuge, D. O., & Gitau, A. N. (2020). Mathematical Modelling, Moisture Transport, Shrinkage and Nutrient Content Properties in Drying Selected African Leafy Vegetables. Applied Engineering in Agriculture, 36(1), 95–104. https://doi.org/10.13031/aea.13532

Nwakuba, N. (2018). A prediction model of energy requirements for drying of okra slices in a hybrid solar-electric Dryer. Journal of Engineering, 4, 144–148.

Nwakuba, N., Ndukwe, S., & Paul, T. (2021). Influence of product geometry and process variables on drying energy demand of vegetables: An experimental study. Journal of Food Process Engineering, 44(6), e13684. https://doi.org/10.1111/jfpe.13684

Nwakuba, N. R. (2019). Optimisation of energy consumption of a solar-electric dryer during hot air drying of tomato slices. Journal of Agricultural Engineering, 50(3), Article 3. https://doi.org/10.4081/jae.2019.876

Putra, R. N., & Ajiwiguna, T. A. (2017). Influence of Air Temperature and Velocity for Drying Process. Procedia Engineering, 170, 516–519. https://doi.org/10.1016/j.proeng.2017.03.082

Sabarez, H. T. (2015). Modelling of drying processes for food materials. In Modelling Food Processing Operations (pp. 95–127). Elsevier. https://doi.org/10.1016/B978-1-78242-284-6.00004-0

Sturm, B., Nunez Vega, A.-M., & Hofacker, W. C. (2014). Influence of process control strategies on drying kinetics, colour and shrinkage of air-dried apples. Applied Thermal Engineering, 62(2), 455–460. https://doi.org/10.1016/j.applthermaleng.2013.09.056

Uzoma, S., Nwakuba, N., & Anyaoha, K. (2020). Response Surface Optimization of Convective Air-Drying Process in a Hybrid PV/T Solar Dryer. Turkish Journal of Agricultural Engineering Research (Turkager), 1(1), 111–130.